

Mapping potential energy landscape of a probing atom in a complex surface environment

Fangfei Ming,¹ Guohua Zhong,² Qin Liu,¹ Kedong Wang,³ and Xudong Xiao^{1,2,*}

¹*Department of Physics, The Chinese University of Hong Kong, Shatin, New Territory, Hong Kong, China*

²*Shenzhen Institute of Advanced Technology, Chinese Academy of Science, Shenzhen, China*

³*Department of Physics, South University of Science and Technology of China, Shenzhen, Guangdong 518055, China*

(Received 26 May 2015; revised manuscript received 12 November 2015; published 30 November 2015)

We have mapped the potential energy landscape for a Ag atom around Ag clusters on Si(111), via positioning a probing atom in the vicinity of clusters and monitoring the subsequent thermal motions with scanning tunneling microscopy. Both the probing atom's modulated diffusion and its combination with the clusters are quantitatively measured in a wide temperature range, showing strong dependence on the cluster size as well as specific sites. The atom-cluster interactions, as large as over 200 meV, are determined and found to alternate between attraction and repulsion at different separations. The demonstrated ability of studying atomic scale dynamics of single adsorbates in complex environments can provide opportunities to understand various phenomena in nanostructure growth and nanocatalysis.

DOI: [10.1103/PhysRevB.92.201414](https://doi.org/10.1103/PhysRevB.92.201414)

PACS number(s): 68.37.Ef, 68.43.Jk, 68.47.Fg, 81.16.Ta

The potential energy landscape of single atoms/molecules in the vicinity of interacting nanostructures and the resultant dynamics are critically important for many subjects of physics, chemistry, and biology. In nanostructure growth [1,2], it dictates various phenomena such as cluster coalescence [3], Ostwald ripening [4], oriented attachment [5], and variations in morphologies [6]. In nanocatalysis, the dynamics of the reacting atom/molecule near the catalytic active sites of nanoclusters controls the reaction rate and even the reaction pathway [7,8]. Quantitative information on such dynamics not only contributes to the understanding of the vast phenomena but further helps develop control on them [9–12]. Conventionally, single-adsorbate dynamics has been obtained in an averaged way by analyzing the resultant morphologies in growth or chemical reaction products [1,8]. Alternatively, tracing individual atom/molecules could provide direct knowledge in the atomic scale [13–15], which is especially important for structure- and site-sensitive properties that prevail in nanoscale materials. Unfortunately, most previous studies on the dynamics of surface adsorbates limit the environment to flat terraces or straight step edges of metal surfaces, and the focus is at most on the interidentical adsorbate interactions [6,16]. Comparing to these relatively ideal cases, experimental study on the interactions in complex environments are still rare. Because of the lack of control in the atomic scale systems, the dynamic behaviors of adsorbates in complex surface structures or at energetically unfavorable configurations could hardly be measured.

In this Rapid Communication, we demonstrate that the complex potential energy landscape of a Ag atom adsorbed near a Ag cluster on a Si(111) – (7 × 7) surface could be mapped by positioning a probing Ag atom to designated sites and tracking its subsequent thermal motions with scanning tunneling microscopy (STM), whose power in atomic resolution imaging and atomic manipulation has been well proven [17–21]. The precise single-atom positioning enables repetitive construction of isolated atom-cluster systems with

identical initial settings as well as controlled environments. They could be far beyond thermal equilibrium and therefore could hardly be produced by thermal growth. The affected diffusion of the probing atom near the cluster and its combination with the cluster were quantitatively measured in a wide temperature range. The atom-cluster interaction energy showed a strong dependence on both cluster size and their specific sites, and manifested alternation between attractive and repulsive substrate-mediated interactions in the distance range before forming a chemical bond.

We prepared a number of Ag clusters on a *n*-type Si(111) – (7 × 7) surface in an ultrahigh vacuum chamber. Silver on Si(111) is a model system for metal cluster growths [22] and the behavior of a single Ag atom on it has been well studied [23,24]. Both the faulted half unit cells (FHUCs) and the unfaulted half unit cells (UHUCs) of Si(111) – (7 × 7) can serve as identical template traps for Ag cluster construction. The Ag clusters could be formed either by thermal growth [22] or by assembly via atomic manipulation [25]. In this study, the latter method was used. We first deposited Ag atoms onto the Si surface by electron-beam evaporation and then used a functionalized STM tip to repetitively transfer Ag atoms in a one-by-one fashion via vertical atom manipulation from elsewhere to a target FHUC trap [25]. Thermal motion of these Ag atoms at room temperature would lead to the formation of a stable Ag cluster with known cluster size through counting the number of Ag atoms used in the assembly. With the sample cooled or heated *in situ* to a designated temperature, a single probing Ag atom was then intentionally transferred to one of the neighboring UHUCs of the constructed cluster, again by vertical atom manipulation. The detailed conditions of the vertical atom manipulation were reported in Ref. [25], which works well between 100 and 340 K in this study. Such operation can well control the zero time of the dynamic observation in addition to controlling the environments by keeping the studied atom-cluster system far away from defects and other Ag atoms and clusters. Two types of dynamic behaviors of the probing Ag atom, one concerning the dynamics within the UHUC and the other concerning the final combination with the cluster, were investigated. Once the probing Ag atom was merged

*Author to whom correspondence should be addressed: xdxiao@phy.cuhk.edu.hk

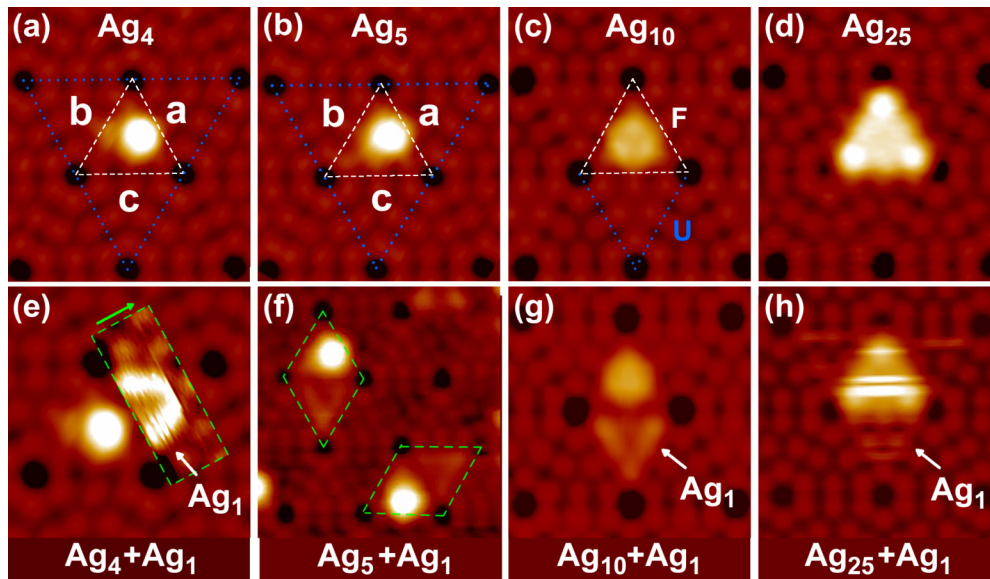


FIG. 1. (Color online) (a–d) STM images showing Ag_4 , Ag_5 , Ag_{10} , and Ag_{25} clusters. “a,” “b,” and “c” label the three nonequivalent UHUCs next to Ag_4 or Ag_5 . (e–h) Examples showing the dynamics of a probing Ag atom next to various Ag clusters. The “F” and “U” in (c) represent FHUC and UHUC, respectively. The dashed rectangle in (e) is a closeup STM image and the arrow at its upper left side shows the scan direction. The fuzzy feature in (h) is a result of the probing Ag atom hopping into and out of the Ag_{25} cluster at a time scale comparable to the STM scan speed. Tunneling conditions for all images: $V_s = +2 \text{ V}$; $I_t = 3 \text{ pA}$.

into the Ag cluster, the dynamic observation was terminated. To increase the statistical events for observation, we took advantage of the atom manipulation to remove one Ag atom from the resultant new Ag cluster and placed the picked Ag atom back into the designated UHUC. In such a manner, identical initial configuration could be repetitively established and new measurement on an identical system with identical environment could be repetitively performed.

We have chosen Ag_4 , Ag_5 , Ag_{10} , and Ag_{25} as representative clusters to study their influence on the dynamics of the probing Ag atom and map their potential energy landscape for the atom. Ag_{10} and Ag_{25} are the most stable clusters and possess geometrically close atom shells [26]. Both of them register well with the substrate and have threefold symmetry, making the three neighboring UHUCs equivalent, as shown in Figs. 1(c) and 1(d). Ag_4 and Ag_5 on the other hand have three nonequivalent neighboring UHUCs which are distinguished by the labels “a,” “b,” and “c” in Figs. 1(a) and 1(b). In the following discussion, the respective UHUCs and the related results will be designated as $\text{Ag}_n\text{-a}$, $\text{Ag}_n\text{-b}$, and $\text{Ag}_n\text{-c}$ ($n = 4, 5$). The different sizes and different shapes of the chosen clusters can provide various manifestations to the dynamics of the probing Ag atom, which can be precisely investigated by the method described above.

Figures 1(e)–1(h) show examples of the dynamics measurement at room temperature. In Fig. 1(e), right after the probing Ag atom was placed in the $\text{Ag}_4\text{-a}$ UHUC, a smaller area was fast imaged at a scan speed of 0.1 s/line. As seen in the inserted rectangular image, the probing Ag atom first randomly hopped within this UHUC, as shown by the time averaged bright features, and then suddenly disappeared from this UHUC to combine with Ag_4 , as recorded by the sudden change of the bright feature. The residence time of the probing Ag atom in this UHUC could be measured by counting the

number of scan lines. In Fig. 1(g), the STM image shows the random motion of the probing Ag atom in one of the neighboring UHUCs of Ag_{10} . The residence time of the probing Ag atom in such a case was much longer and could be measured by counting the number of image frames, and multiple events could be monitored at the same time, as shown by the two $\text{Ag}_5\text{-b} + \text{Ag}_1$ in Fig. 1(f). Figure 1(h) shows the fast combination of the probing Ag atom with Ag_{25} and the spontaneous dissociation of the produced Ag_{26} , as implied by the fuzzy features. By exploiting the spontaneous dissociation of Ag_{26} into an Ag_{25} and a neighboring Ag atom, we here no longer needed to use atom manipulation to repetitively create the identical initial configuration. The residence time of the probing Ag atom in the UHUC next to Ag_{25} could be measured by the time-dependent current spectroscopy [27], in which the STM tip was placed stationary above this UHUC and the appearance and absence of the probing Ag atom in the UHUC were reflected by different tunneling current levels. In contrast to imaging, the time-dependent current spectroscopy allowed a residence time measurement shorter than 1 ms (see the Supplemental Material [28]).

The dynamics of combination of the probing Ag atom with the neighboring cluster can be represented by the temperature-dependent residence time in the concerned UHUCs. The results are plotted in the Arrhenius form in Fig. 2. As a comparison, the free inter-half-cell hopping result of the probing Ag atom from a UHUC into a neighboring FHUC with no Ag cluster around is also plotted and labeled as “free.” Each data point in Fig. 2 represents an average of 10–100 measured combination events. The highest temperature for $\text{Ag}_4\text{-c}$ was limited to 340 K in order to avoid thermal change of Ag_4 orientation, which rendered the three nonequivalent neighboring UHUCs meaningless. We use $1/\tau = \nu_0 \exp(-E_a/kT)$ to fit each set of data and the deduced activation energy E_a and prefactor ν_0 are

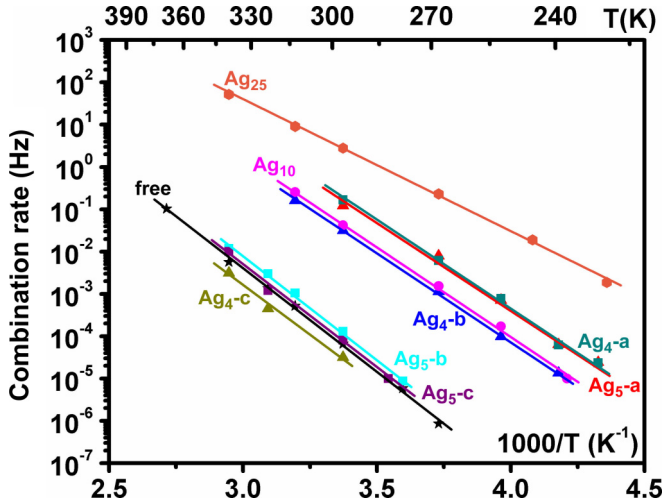


FIG. 2. (Color online) Arrhenius plot of the combination rate for the probing Ag atom to combine with the neighboring Ag₄, Ag₅, Ag₁₀, or Ag₂₅ clusters. Together is plotted the inter-half-cell hopping rate of a free Ag atom from a UHUC to a neighboring FHUC away from defects and other Ag atoms or clusters.

summarized in Table I. The good fitting quality verifies that the measured processes come from thermal excitation.

It is clear from Fig. 2 that at a given temperature the combination rate in many cases is orders of magnitude faster than the free inter-half-cell hopping rate. These results demonstrate that the Ag clusters in the neighboring FHUC greatly influence the combination process and both their sizes and orientations play an indispensable role. Table I provides quantitative comparison between the clusters and the free hopping: Ag₄ and Ag₅ seem not to influence E_a for Ag₄-c, Ag₅-b, and Ag₅-c much, but substantially reduce E_a for Ag₄-a, Ag₄-b, and Ag₅-a by 170, 140, and 150 meV, respectively. Ag₁₀ and Ag₂₅ also reduce E_a by 130 and 350 meV each. Such results imply that the Ag clusters attract the neighboring Ag atoms, consistent with previous reports [22,29,30]. Qualitatively, the closer the cluster is to the probing Ag atom, the lower the activation energy. Between Ag₂₅ and Ag₁₀, since the former occupies not only the inner but also the outer shell sites, it lowers E_a more. For Ag₄, the average distance between the cluster and the probing Ag atom in Ag₄-c, Ag₄-b, and Ag₄-a progressively decreases [Fig. 1(a)], and so does E_a . A similar claim can be qualitatively made for Ag₅. Within the experimental uncertainty, ν_0 does not seem to change much from the free case of $10^{12.2}$ Hz, except that a clear decrease to $10^{10.9}$ Hz for Ag₂₅ is observed.

The effect of the clusters on the intra-UHUC hopping of the probing Ag atom can be well demonstrated by low-temperature images in Figs. 3(a)–3(e), in which the free hopping is also shown for comparison. Away from the cluster by just one unit

cell, the hopping of the probing Ag atom already recovers the threefold symmetry [“free” in Fig. 3(d)], indicating negligible interaction by the cluster. In contrast, the hopping behavior of the probing Ag atom is clearly modified by the neighboring cluster. The center image spots at the edge of Ag₄-a, Ag₄-b, and Ag₁₀-UHUC next to the clusters clearly become dimmer, whereas the according corner image spots of Ag₁₀-UHUC are obviously brighter. For Ag₂₅, we had to image at 1 V to better view the probing Ag atom [Fig. 3(e)]. It can be seen that the full edge of UHUC next to Ag₂₅ becomes almost transparent so that the three underlying Si adatoms clearly appear in the image. The observed brightness changes indicate that the probing Ag atom is repelled from the sites related to the dimmer spots, but attracted to the sites related to the brighter spots. The quantitative measurement will be detailed in the later parts.

To quantitatively evaluate the adsorption energy change ΔE of the probing Ag atom due to the interaction of the clusters, we used time-dependent tunneling spectra to record the site-specific occupancy at 100 K and employed the relation that the ratio of site occupancy is proportional to $\exp(\Delta E/kT)$ to calculate ΔE for each site (Supplemental Material [28]). At such low temperature, the inter-HUC hopping measured above 225 K in Fig. 2 would be completely frozen out, whereas the intra-HUC hopping is slowed down to a measurable range. As shown in Figs. 3(f)–3(h), there are nine adsorption sites where the probing Ag atom can reside within the UHUC [22]. In a clean environment, these nine adsorption sites have almost equal adsorption energy, with about 4.5 meV less on sites near the center Si adatoms than on sites near the corner Si adatoms, consistent with previous results [24]. Shown in Figs. 3(f)–3(h) are the measured results of ΔE at each site for clusters Ag₄, Ag₁₀, and Ag₂₅, respectively. While the ΔE values at sites far enough from the clusters become negligible (<10 meV), they show significant changes at sites neighboring the clusters. There is an obvious effect from cluster size as well as from orientation; both of them alter the distance between the probing Ag atom and the clusters. For Ag₂₅, the four adsorption sites near the cluster show a dramatic adsorption energy decrease, which reduces the frequency with which the probing Ag atom visits them. Such an occupancy change has a direct consequence to the prefactor of combination rate since it is expected that the probing Ag atom must diffuse to Ag₂₅ via one of these four sites. The deduced decrease of $10^{1.3}$ in ν_0 for combination with Ag₂₅ compared to the free case in Table I directly reflects such an effect. In contrast, for Ag₄, Ag₅, and Ag₁₀, the clusters only repel the probing Ag atom at the two sites near the center Si adatom but slightly attract it at the other two sites near the corner Si adatoms. Presumably, the probing Ag atom can combine with the related clusters via these corner sites and thus slightly increases (not discernible from experimental errors) their respective prefactors.

TABLE I. Fitted activation energy E_a and prefactor ν_0 for data in Fig. 2. The values for ν_0 are the respective exponent k .

| | Free | Ag ₄ -a (Ag ₅ -a) | Ag ₄ -b (Ag ₅ -b) | Ag ₄ -c (Ag ₅ -c) | Ag ₁₀ | Ag ₂₅ |
|------------------|----------------|---|---|---|------------------|------------------|
| E_a (meV) | 970 ± 20 | 800 ± 50 (820 ± 30) | 830 ± 50 (960 ± 60) | 910 ± 150 (980 ± 70) | 840 ± 40 | 620 ± 20 |
| $\nu_0(10^k$ Hz) | 12.2 ± 0.6 | 12.7 ± 0.8 (13.2 ± 0.8) | 12.5 ± 0.8 (12.5 ± 1.0) | 11.0 ± 2.0 (12.2 ± 1.0) | 13.0 ± 0.8 | 10.9 ± 0.6 |

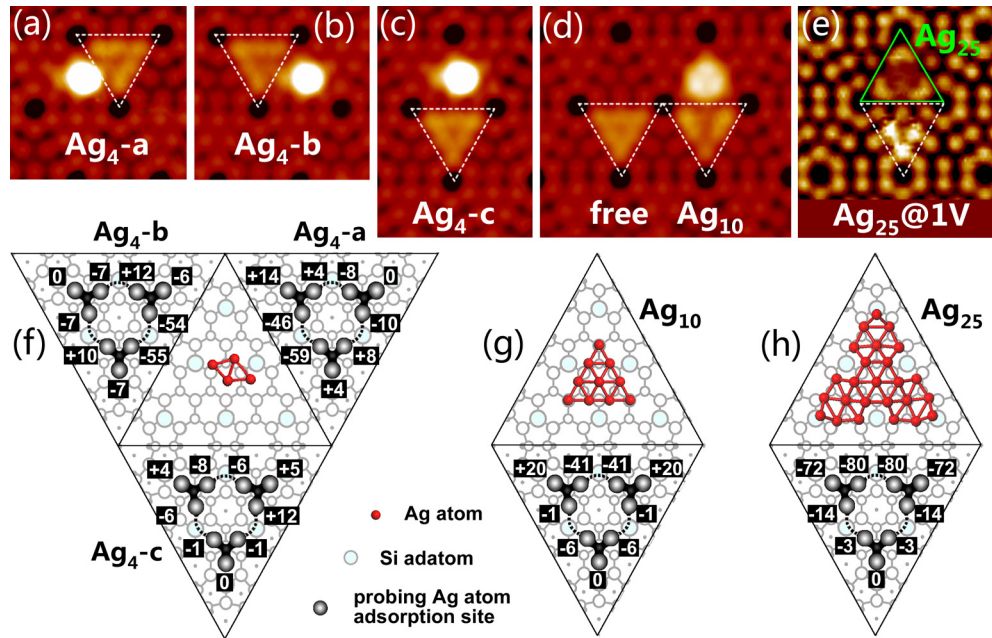


FIG. 3. (Color online) (a–e) STM images showing the intra-UHUC hopping of the probing Ag atom influenced by the nearby Ag clusters. All traces of the probing Ag atom are highlighted by dashed triangles. The imaging conditions are +2 V at 175 K for (a–d) and +1 V at 155 K for (e). An unaffected Ag atom moving in a UHUC is also displayed in (d). (f,g) The deduced adsorption energy changes ΔE (in meV) of the probing Ag atom at the given sites in the neighboring UHUCs, together with the density functional theory optimized models of Ag₄, Ag₁₀, and Ag₂₅.

Figure 4(a) elaborates the interaction and the dynamics of the atom-cluster system: Inside the UHUC next to the cluster, the probing Ag atom hops quickly among various adsorption sites. The repulsion due to the cluster reduces the adsorption energy of the probing Ag atom at site(s) (labeled with “1”) next to the cluster, in particular, at sites near the center Si adatom. At the boundary between two neighboring UHUCs, the attraction due to the cluster, however, lowers the saddle point (possibly the site labeled “2” [22]) barrier energy for combination. For Ag₂₅, the probing Ag atom at the saddle point

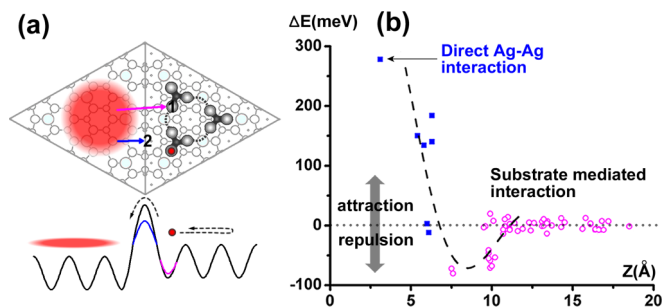


FIG. 4. (Color online) (a) Sketch of a probing Ag atom next to a Ag cluster. Two solid arrows show the distance from the cluster to the adsorption site “1” and to the saddle site “2” of the probing Ag atom. The black curve in the lower panel sketches the original energy landscape of the probing Ag atom and the blue and pink curves sketch the modulated energy landscape due to the cluster. (b) The deduced energy change ΔE versus separation. Circles are results from the adsorption sites inside the UHUC next to the clusters, and squares are results from the inter-half-cell barrier sites. Positive value represents “attraction,” and negative value represents “repulsion.” The dashed line is a guide to the eye.

is ~ 3.1 Å away from the cluster edge Ag atom, comparable with the Ag-Ag bond length of 2.88 Å, and can possibly interact directly with the cluster Ag atom to provide strong attraction—but for Ag₄, Ag₅, and Ag₁₀, the probing Ag atom at the saddle point is still far away from any Ag atoms in these clusters and cannot significantly directly interact with the cluster Ag atoms. The reduction of barrier energy must dominantly originate from the substrate-mediated interaction. Without getting into the detailed structural dependence, we plot in Fig. 4(b) the deduced ΔE as a function of atom-cluster separation, defined by the distance between the position of the probing Ag atom and the closest cluster Ag atom (Figs. 3(f)–3(h) and Supplemental Material [28]). It should be noted that the atom-cluster separations are largely determined by the apparent configurations in the STM images and therefore should not be sensitive to detailed atomic models. As seen from the data, as the separation increases, ΔE starts with attraction below 6 Å, decays and changes sign to repulsion before 10 Å, and becomes small in magnitude and featureless afterwards. The initial oscillating behavior is reminiscent of Friedel oscillations between adsorbates on metal surfaces mediated by free-electron-like surface bands [16]. For Si(111) – (7 × 7) substrate with its electrons in the surface bands near the Fermi level practically localized on adatoms, the mechanism of substrate mediation may be different and demands further investigation. It is likely that the charge redistribution and/or lattice relaxations induced by the cluster give rise to the short-range and alternating interactions.

In summary, we used atomic manipulation to position single probing Ag atoms to the vicinal sites of Ag clusters to construct identical as well as energetically unstable atom-cluster configurations on Si(111) – (7 × 7). Quantitative

measurement on the thermal motions of the probing atom revealed the complex potential energy landscapes of a Ag atom adsorbed near Ag clusters. This is a viable study of atomic motions in an arbitrary environment on a nonmetal surface. In the future, not only the complex environment can be extended to arbitrary nanostructures, irregularly shaped or composed of different elements on the same substrate, but also the demonstrated methods and results are expected to have broad applicability in studies on atom/molecule dynamics near other complex nanostructures considering a large variety

of atoms/molecules has been reported to be manipulable on different surfaces. This will further advance our understanding of various physical and chemical processes in an atomic view.

This work was supported by the Chinese University of Hong Kong (Focused Research Scheme B and Direct Grant for Research), the Research Grants Council of Hong Kong (Grant No. 403311), and the MOST 973 Program (Grant No. 2014CB921402).

-
- [1] Z. Y. Zhang and M. G. Lagally, *Science* **276**, 377 (1997).
 [2] J. A. Elemans, S. Lei, and S. De Feyter, *Angew. Chem., Int. Ed.* **48**, 7298 (2009).
 [3] J. M. Zuo and B. Q. Li, *Phys. Rev. Lett.* **88**, 255502 (2002).
 [4] L. Ratke and P. W. Voorhees, *Growth and Coarsening: Ostwald Ripening in Material Processing* (Springer-Verlag, New York, 2002).
 [5] D. Li, M. H. Nielsen, J. R. Lee, C. Frandsen, J. F. Banfield, and J. J. De Yoreo, *Science* **336**, 1014 (2012).
 [6] T. Michely and J. Krug, *Islands, Mounds and Atoms: Patterns and Processes in Crystal Growth Far from Equilibrium* (Springer-Verlag, New York, 2004).
 [7] D. K. Böhme and H. Schwarz, *Angew. Chem., Int. Ed.* **44**, 2336 (2005).
 [8] I. X. Green, W. Tang, M. Neurock, and J. T. Yates, Jr., *Science* **333**, 736 (2011).
 [9] C. Misbah, O. Pierre-Louis, and Y. Saito, *Rev. Mod. Phys.* **82**, 981 (2010).
 [10] R. Ganapathy, M. R. Buckley, S. J. Gerbode, and I. Cohen, *Science* **327**, 445 (2010).
 [11] C. Y. Chiu, Y. Li, L. Ruan, X. Ye, C. B. Murray, and Y. Huang, *Nat. Chem.* **3**, 393 (2011).
 [12] H. Zhang, T. Watanabe, M. Okumura, M. Haruta, and N. Toshima, *Nat. Mater.* **11**, 49 (2012).
 [13] B. S. Swartzentruber, *Phys. Rev. Lett.* **76**, 459 (1996).
 [14] T. Mitsui, M. K. Rose, E. Fomin, D. F. Ogletree, and M. Salmeron, *Science* **297**, 1850 (2002).
 [15] K. Kyuno and G. Ehrlich, *Phys. Rev. Lett.* **81**, 5592 (1998).
 [16] P. Han and P. S. Weiss, *Surf. Sci. Rep.* **67**, 19 (2012).
 [17] J. A. Stroschio and R. J. Celotta, *Science* **306**, 242 (2004).
 [18] T. Kumagai, F. Hanke, S. Gawinkowski, J. Sharp, K. Kotsis, J. Waluk, M. Persson, and L. Grill, *Nat. Chem.* **6**, 41 (2014).
 [19] D. H. Lee and J. A. Gupta, *Science* **330**, 1807 (2010).
 [20] B. Wolter, Y. Yoshida, A. Kubetzka, S. W. Hla, K. von Bergmann, and R. Wiesendanger, *Phys. Rev. Lett.* **109**, 116102 (2012).
 [21] C. L. Chiang, C. Xu, Z. Han, and W. Ho, *Science* **344**, 885 (2014).
 [22] I. Ošťádal, P. Kocán, P. Sobotík, and J. Pudl, *Phys. Rev. Lett.* **95**, 146101 (2005).
 [23] P. Sobotík, P. Kocán, and I. Ošťádal, *Surf. Sci.* **537**, L442 (2003).
 [24] K. Wang, G. Chen, C. Zhang, M. M. T. Loy, and X. Xiao, *Phys. Rev. Lett.* **101**, 266107 (2008).
 [25] F. Ming, K. Wang, S. Pan, J. Liu, X. Zhang, J. Yang, and X. Xiao, *ACS Nano* **5**, 7608 (2011).
 [26] F. Ming, G. Zhong, Q. Liu, K. Wang, Z. Zhang, and X. Xiao, *Phys. Rev. B* **88**, 125432 (2013).
 [27] K. Wang, C. Zhang, M. M. T. Loy, and X. Xiao, *Phys. Rev. Lett.* **94**, 036103 (2005).
 [28] See Supplemental Material at <http://link.aps.org/supplemental/10.1103/PhysRevB.92.201414> for the details of measuring the inter-HUC hopping of the probing Ag atom and the adsorption energy change ΔE at each adsorption site.
 [29] Y. Sugimoto, A. Yurtsever, N. Hirayama, M. Abe, and S. Morita, *Nat. Commun.* **5**, 4360 (2014).
 [30] F. Ming, K. Wang, X. Zhang, J. Liu, A. Zhao, J. Yang, and X. Xiao, *J. Phys. Chem. C* **115**, 3847 (2011).